

2-23-2022

## Optimal curing humidity for compacted bentonite-sand mixtures

Hu-yuan ZHANG

*Key Laboratory of Mechanics on Disaster and Environment in Western China of Ministry of Education, Lanzhou University, Lanzhou, Gansu 730000, China*

Zhi-nan DING

*School of Civil Engineering and Mechanics, Lanzhou University, Lanzhou, Gansu 730000, China;*

Yu TAN

*School of Civil Engineering and Mechanics, Lanzhou University, Lanzhou, Gansu 730000, China;*

Jiang-hong ZHU

*School of Civil Engineering and Mechanics, Lanzhou University, Lanzhou, Gansu 730000, China;*

*See next page for additional authors*

Follow this and additional works at: <https://rocksoilmech.researchcommons.org/journal>



Part of the [Geotechnical Engineering Commons](#)

---

### Custom Citation

ZHANG Hu-yuan, DING Zhi-nan, TAN Yu, ZHU Jiang-hong, CAO Zhi-wei, . Optimal curing humidity for compacted bentonite-sand mixtures[J]. Rock and Soil Mechanics, 2021, 42(11): 2925-2933.

This Article is brought to you for free and open access by Rock and Soil Mechanics. It has been accepted for inclusion in Rock and Soil Mechanics by an authorized editor of Rock and Soil Mechanics.

---

## Optimal curing humidity for compacted bentonite-sand mixtures

### Authors

Hu-yuan ZHANG, Zhi-nan DING, Yu TAN, Jiang-hong ZHU, and Zhi-wei CAO

## Optimal curing humidity for compacted bentonite-sand mixtures

ZHANG Hu-yuan<sup>1,2</sup>, DING Zhi-nan<sup>1</sup>, TAN Yu<sup>1</sup>, ZHU Jiang-hong<sup>1</sup>, CAO Zhi-wei<sup>1</sup>

1. School of Civil Engineering and Mechanics, Lanzhou University, Lanzhou, Gansu 730000, China;

2. Key Laboratory of Mechanics on Disaster and Environment in Western China of Ministry of Education, Lanzhou University, Lanzhou, Gansu 730000, China

**Abstract:** The buffer blocks used in deep geological repositories of high-level radioactive wastes (HLW) should be cured in an appropriate environment to prevent the deterioration of buffer blocks such as desiccation shrinkage and cracking. In this study, the bentonite-sand mixtures with different initial moisture contents (11.23–21.63%) were compressed in the laboratory to simulate the production of buffer blocks. The bentonite-sand mixtures were cured at different relative humidity (*RH*) of 33%, 75%, 85% and 100% in order to find the optimum curing humidity. During the curing process, the periodical mass change was weighed by a balance, the size change was measured by a vernier caliper, and the thermal conductivity was tested after the curing was balanced. The test results indicate that the moisture variation of bentonite-sand mixtures during curing was consistent with the soil-water characteristic curves (SWCCs) of the mixtures. When the compacted bentonite-sand mixtures were cured at the relative humidity of 33%, 75% and 85%, the samples were dehydrated and became dried, resulting in desiccation shrinkage and cracking. When the relative humidity was 100%, the mixtures with a lower initial moisture content of 11.23–14.99% tended to absorb moisture from the environment and swelled. While the mixtures with a higher moisture content of 17.22–21.63% were desiccated to shrink, but no obvious cracks were observed on the surface of these cured specimens. Under the curing condition of *RH* = 100%, the variation of water content and volume of the sample with an initial water content of 17.22% was the minimum, which was considered as the optimum curing humidity for buffer blocks. The optimal curing conditions (optimum *RH*) of industrial-scale buffer blocks used in the disposal repository can be estimated by the SWCCs of the small buffer blocks, and the development of drying shrinkage crack can be quantitatively evaluated by the thermal conductivity of buffer blocks.

**Keywords:** high-level radioactive waste (HLW); bentonite-sand mixture; buffer block; curing; relative humidity

### 1 Introduction

High-level radioactive waste (HLW) disposal repository is a multi-barrier system<sup>[1]</sup>. Currently, the compacted block masonry method is the mainstream method for buffer barrier design of HLW disposal repositories<sup>[2]</sup>. The preparation of buffer blocks generally adopts special equipment to compress buffer materials with a certain moisture content to the maximum dry density. The compacted blocks undergo the process of preservation and transportation prior to installation in the underground disposal repository, during which they might experience changes in ambient temperature and humidity. Bentonite materials are very sensitive to the change of moisture content. Drying and water loss will produce shrinkage cracking<sup>[3]</sup>, while when they absorb water, the cracking caused by the expansion will occur<sup>[4]</sup>. Therefore, some curing measures should be taken to protect the buffer blocks during storage to ensure their quality.

Experience from underground laboratory tests has shown that the installation time of buffer blocks in the underground disposal repository is approximately three months<sup>[5]</sup>. Depending on the design of disposal roadways, groundwater flows along the tunnel floor throughout the construction period, and the humidity in the tunnel may approach 100%<sup>[6]</sup>. Hence, the buffer block needs to have a high initial moisture content to prevent it from absorbing water from the high humidity environment

of the disposal roadway during installation, resulting in the cracking of the block due to expansion and thus affecting the stability and accuracy of the buffer block installation<sup>[4]</sup>. However, the construction site of China's underground laboratories for geological disposal of high-level radioactive waste is located in the Xinchang section of Beishan district, Gansu Province<sup>[7]</sup>, which belongs to a typical continental climate. In this area, the average environmental humidity for many years is about 37.08% and the average temperature is about 7.60 °C<sup>[8]</sup>. During the production and storage of buffer blocks in this area, they will be exposed to a relatively dry environment. If the initial moisture content of the block is high, dehydration will inevitably occur. Therefore, it is necessary to strictly control the humidity of the environment during the storage of buffer blocks to prevent the drying and deterioration of blocks.

Previous studies on block curing have shown that environmental humidity is one of the most important indexes in the storage process of buffer blocks. Tan et al.<sup>[3]</sup> exposed the buffer blocks to indoor environmental conditions without controlling the environmental humidity, and they found that a large number of drying cracks appeared on the block surface within a few hours. Peter<sup>[6]</sup> studied the relationship between the distribution of moisture content and dry density of bentonite blocks and the development of cracks under the change of humidity. He found that the external dry

Received: 13 May 2021

Revised: 26 July 2021

This work was supported by the National Natural Science Foundation of China (41972265).

First author: ZHANG Hu-yuan, male, born in 1963, PhD, Professor, Doctoral supervisor, mainly engaged in the teaching and research of environmental geotechnical engineering related to waste disposal. E-mail: zhanghuyuan@lzu.edu.cn

density was higher than the internal one after the block was dried, and the number and depth of cracks increased with time. By studying the moisture absorption rate and expansion deformation of bentonite samples in the atmosphere, Lars Erik<sup>[9]</sup> found that the moisture absorption rates of bentonite samples with different dry densities were roughly the same. Benoit et al.<sup>[10]</sup> pointed out that compacted bentonite blocks were very sensitive to environmental humidity, and too high or too low environmental humidity would lead to block deterioration. Therefore, the ambient humidity around the buffer block should be well controlled at all stages (i.e., preparation, storage, transportation, and installation)<sup>[11]</sup>. The above existing research results show that the control of environmental humidity is the key factor to prevent block deterioration. However, at present, there is no optimum scheme of block curing for the blocks used in the HLW disposal repository in China, which hinders the construction process of the underground laboratory for geological disposal of high-level radioactive waste in the Beishan district of China.

In order to find an optimum curing scheme for high-tension buffer blocks, this study employed the common preparation method of buffer blocks to make buffer blocks indoors and tested the variation of physical state and thermal conductivity under different environmental humidity conditions. The curing humidity referred to the low humidity environment in the Beishan district and the high humidity environment in the underground HLW disposal repository. According to the moisture content change, the volume change, and the crack development of buffer blocks under different environmental humidity, the range of the optimal curing humidity of buffer blocks was determined, providing technical and data support for subsequent research on block curing.

## 2 Testing materials and methods

### 2.1 Testing materials

According to the preparation method and material of the hybrid buffer block for high-level radioactive waste disposal in China, some small compacted samples were made in the laboratory. In compacting buffer blocks, the dry density of the block could be controlled by changing the dry mass and moisture content of the block and compaction stress<sup>[12–14]</sup>. The bentonite used to prepare hybrid buffer blocks was Gaomiaozi sodium bentonite (GMZ bentonite) from Xinghe County, Inner Mongolia, and the quartz sand was the standard sand processed from Yongdeng quartzite in Gansu province, China. Since the same materials and sample preparation methods were used in this work, the sand mixing rate was determined based on the fuzzy comprehensive evaluation<sup>[15]</sup>. The dry mass ratio of the two materials in the bentonite sand mixture was 70% GMZ bentonite and 30% quartz sand. The basic physical properties of the two testing materials are shown in Table 1.

**Table 1 Basic physical properties of testing materials**

Materials	Relative density	Particle size /mm	Liquid limit /%	Plastic limit /%	Moister content after air drying /%
GMZ	2.70	<0.075	152	28	9.56
GMZ Bentonite					
Quartz sand	2.65	0.5–2.0	—	—	0

### 2.2 Sample preparation

The preparation of buffer blocks in China is based on the compaction curve of materials<sup>[16]</sup>. In order to simulate the curing of buffer blocks in different compaction states, basically, the whole compaction curves of the block were used for sample preparation in this paper to study the initial state of different blocks (see Table 2 for sample design and Fig. 1 for sample compaction parameters). Based on the existing studies, the bentonite-sand mixture samples studied in this paper were all in the high suction part, and the dry density had little effect on the moisture holding capacity of the samples. Therefore, the effect of the different dry densities of samples selected in this work on their water holding capacity could be ignored.

**Table 2 Design of the samples**

No.	Moisture content /%		Dry density /( $\text{g} \cdot \text{cm}^{-3}$ )		Saturation degree /%	Height /cm	Diameter /cm
	Target value	Measured value	Target value	Measured value			
W1	11.00	11.23	1.83	1.81	62.6	2.23	5.00
W2	13.00	13.23	1.86	1.84	77.7	2.19	5.00
W3	15.00	14.99	1.80	1.83	86.5	2.26	5.00
W4	17.00	17.22	1.70	1.72	82.7	2.40	5.00
W5	21.00	21.63	1.60	1.64	91.4	2.55	5.00

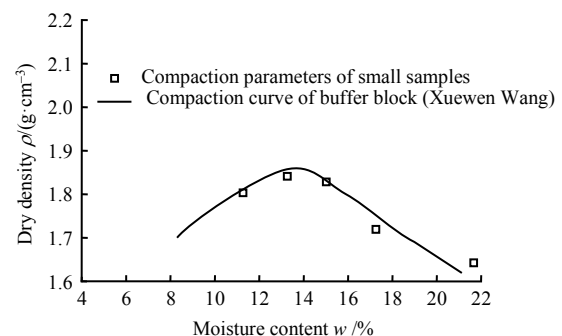


**Fig. 1 Parameters for sample compaction**

The specific sample preparation procedures were as follows: Firstly, the air-dried bentonite and quartz sand were fully stirred and mixed according to the dry mass ratio of 7:3. Then, the distilled water with designed quality was sprayed into the evenly mixed bentonite-sand mixture by spraying method, and the water was evenly distributed by sufficient stirring. After that, the bentonite-sand mixture was placed in an airtight bag and placed in a humidifier for 60 hours to achieve uniform moisture wetting. After the wetting, the bentonite-sand mixture with a dry weight of 80 g was poured into a special cylindrical compaction mould, which was then pressed to the target volume by the volume control method. The load was maintained at

about 20 MPa for 1 minute, after which the bentonite-sand mixture was unloaded and demoulded. After demoulding, the sample was immediately weighed and measured for height and diameter, then stored in an airtight bag. After the testing sample was pressed, the sample was moved to the dryer with the saturated salt solution at the bottom to carry out the next curing test. Under this compaction condition, the thickness of the samples with different initial moisture contents would have a certain difference, which would affect the time required for the process of moisture absorption and dehumidification, but the influence on the final moisture content was very limited.

### 2.3 Testing methods

The water vapour equilibrium method was adopted to control the curing humidity in the curing test, that is, the specific saturated vapour pressures formed by different saturated salt solutions were used to control the relative humidity of water vapour in the container<sup>[18]</sup>. Distilled water was used to control the curing humidity environment with a relative humidity of 100%. The sample was placed on the clapboard with holes in the desiccator with the saturated salt solution below the sample (see Fig. 2). The internal temperature of the laboratory was controlled by air conditioning facilities and maintained at  $22 \pm 1^\circ\text{C}$ .

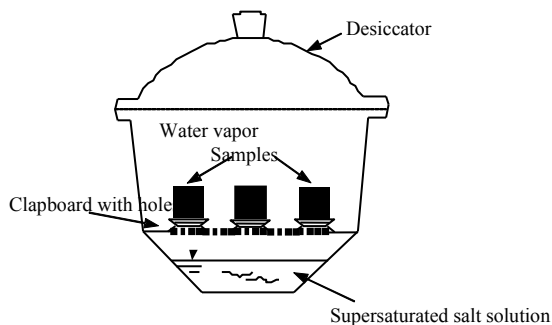


Fig. 2 Schematic diagram of the water vapor equilibrium method

Considering the low humidity environment in Beishan, Gansu province (37.08%) and the possible high humidity environment in the underground disposal repository (100%), the preparation and installation of buffer blocks might experience the above two humidity conditions. Hence, based on these two extreme humidity conditions, four different humidity levels were designed in this work (see Table 3), namely 33%, 75%, 85% and 100%. Under each curing humidity condition, three samples with the same initial moisture content were set up for parallel tests to verify the repeatability of the results.

After the simulated curing test began, the changes of the mass, diameter and height of samples during curing were measured regularly, and the development of cracks was recorded by photographing. At a certain time interval, the sample was weighed, and the real-time moisture content of the sample was calculated according to the sample mass and the initial moisture

content.

Table 3 Saturated salt solution used in the test and its controlled relative humidity (22°C)

Saturated salt solution	Relative humidity of steam /%
MgCl <sub>2</sub>	33
NaCl	75
KCL	85
Distilled water	100

The change of moisture content is  $\Delta w$ , i.e.,

$$\Delta w = w_0 - w \quad (1)$$

where  $w_0$  and  $w$  are the initial moisture content and the moisture content at a certain time of the sample, respectively. If  $\Delta w$  is a positive value, this means that the moisture content decreases and the evaporation process of the sample occurs; if  $\Delta w$  is a negative value, this indicates that the moisture content increases and the moisture absorption process of the sample occurs.

A vernier caliper was used to measure the change in sample size. The diameter and height were measured at four different positions, respectively, and the average value was taken. The real-time volume of the sample was calculated according to the average diameter and height of the sample. In order to analyze the dependence between volume change and moisture content change, the volumetric strain rate of the sample was defined as  $\beta$ , as below:

$$\beta = \frac{V - V_0}{V_0} \times 100\% \quad (2)$$

where  $V_0$  and  $V$  are the initial volume and the volume at a certain time of the sample, respectively.  $\beta < 0$  represents the volume shrinkage of the sample,  $\beta > 0$  represents the volume expansion of the sample.

In order to avoid the influence of the external environment on the sample, the sample weighing and the measurement of diameter and height should be done quickly. When the change in the mass of the sample is less than 0.01g within two days<sup>[19]</sup>, it can be considered that the sample has reached equilibrium at this curing humidity.

In order to quantitatively evaluate the crack development of the samples, the thermal conductivity of the bentonite-sand mixture samples was measured before curing and after curing using the Swedish Hot Disk TPS 2500 s constant thermal analyzer. The single side method was used to test the thermal conductivity of the sample in this work. Specifically, the sample was fixed on the bracket, three measuring points were selected on the upper surface of each sample, and each measuring point was tested once with an interval of 2 minutes. The data with large deviations were excluded, and the average value was calculated as the thermal conductivity of the corresponding sample.

### 3 Results and discussions

#### 3.1 Change of moisture content before and after curing

The moisture content of bentonite-sand mixture samples under different curing humidity mainly changed in the first two months of curing, and the curing equilibrium of all samples took about 3 months. The time required for mixture samples to reach moisture

equilibrium increased with the increase of curing humidity. Under the same curing humidity condition, the higher the initial moisture content of the sample, the higher the stable moisture content will be after curing equilibrium. According to the moisture content and volume of the sample before and after curing, as well as Eqs. (1) and (2), the change of moisture content and volumetric strain rate of the sample can be calculated, as shown in Table 4.

**Table 4 Basic parameters, moisture content changes, and volumetric strain rate of the samples before and after curing**

No.	Initial moisture content $w_0$ /%	Initial volume $V_0$ /cm <sup>3</sup>	RH=33%				RH=75%				RH=85%				RH=100%			
			Equilibrium moisture content $w_e$ /%	Change of moisture content $\Delta w$ /%	Equilibrium volume $V_e$ /cm <sup>3</sup>	Volumetric strain rate $\beta$ /%	Equilibrium moisture content $w_e$ /%	Change of moisture content $\Delta w$ /%	Equilibrium volume $V_e$ /cm <sup>3</sup>	Volumetric strain rate $\beta$ /%	Equilibrium moisture content $w_e$ /%	Change of moisture content $\Delta w$ /%	Equilibrium volume $V_e$ /cm <sup>3</sup>	Volumetric strain rate $\beta$ /%	Equilibrium moisture content $w_e$ /%	Change of moisture content $\Delta w$ /%	Equilibrium volume $V_e$ /cm <sup>3</sup>	Volumetric strain rate $\beta$ /%
W1	11.23	43.79	5.50	5.73	42.61	-2.68	9.47	1.76	43.14	-1.47	10.43	0.80	43.41	-0.87	16.49	-5.26	47.88	9.34
W2	13.23	43.00	5.77	7.46	41.78	-2.84	9.83	3.40	41.87	-2.64	10.98	2.25	41.93	-2.49	16.96	-3.73	44.57	3.64
W3	14.99	44.37	5.85	9.14	42.52	-4.18	9.93	5.06	42.60	-4.00	11.05	3.94	42.76	-3.65	16.94	-1.95	45.93	3.50
W4	17.22	47.12	5.96	11.26	44.31	-5.98	9.99	7.23	44.72	-5.11	11.10	6.12	44.72	-5.10	16.87	0.35	46.98	-0.31
W5	21.63	50.07	6.13	15.50	44.58	-10.96	10.28	11.35	44.92	-10.29	11.62	10.01	45.17	-9.78	17.53	4.10	47.13	-5.88

The relationship between the initial moisture content (solid column) and the equilibrium moisture content (diagonal column) of bentonite-sand mixture samples and curing humidity is shown in Fig. 3. The values marked on the dotted line in Fig. 3 represent the range of equilibrium moisture content finally reached by the samples with 5 different initial water content under specific curing humidity conditions. For example,  $w = 5.85 \pm 0.50\%$  indicates that when the curing humidity was 33%, the equilibrium moisture content of the sample ranged from  $5.85 - 0.50\%$  to  $5.85 + 0.50\%$ . It can also be found from Fig. 3 that although the initial moisture content of the samples varied greatly, the moisture content of the samples was nearly uniform after reaching equilibrium at a specific curing humidity, which was consistent with the finding that the dry density of the sample had little effect on the water holding capacity of the sample. The equilibrium moisture content of the sample increased with the increase of curing humidity. Under the same curing humidity, after reaching equilibrium, the equilibrium moisture content of the sample with a high initial moisture content was slightly higher than that of the sample with a low initial moisture content, indicating that there was a certain lag in the process of moisture absorption and dehumidification of bentonite-sand mixture samples<sup>[20]</sup>.

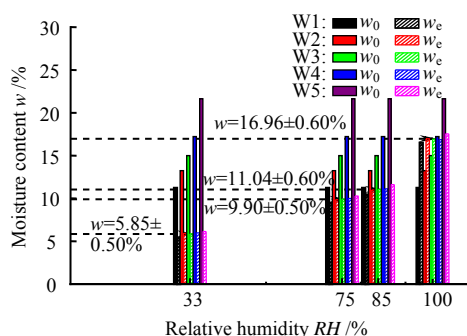


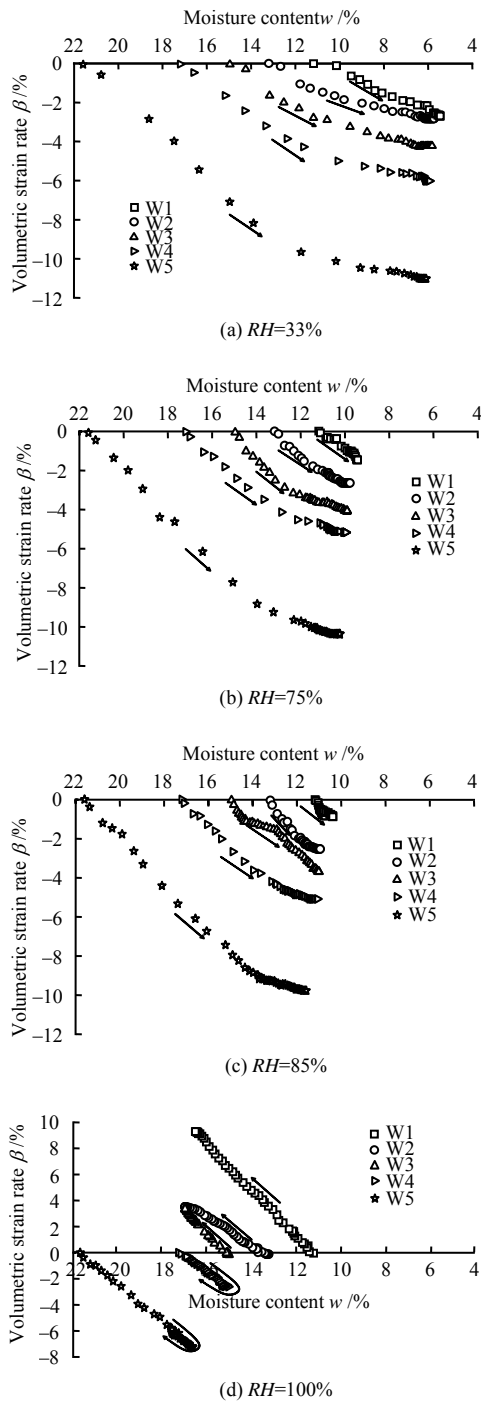
**Fig. 3 Relationship between equilibrium moisture content and curing relative humidity**

#### 3.2 Change of volume before and after curing

The change of moisture content of the bentonite-sand mixture sample will also cause the change of the sample volume. Fig. 4 shows the variation of the volumetric strain rate of samples with moisture content. It can be seen in Fig. 4 that the volumetric strain rate of samples was positively correlated with the change of moisture content, that is, the greater the change of moisture content of the sample was, the greater the volumetric strain rate would be.

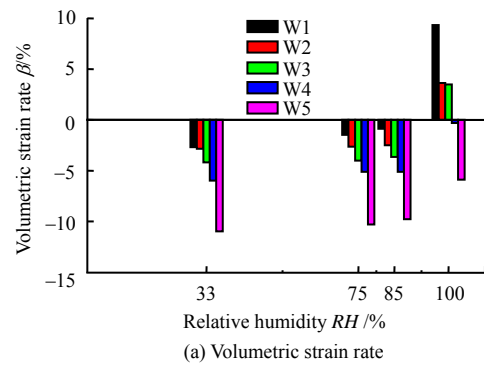
It can be seen from Figs. 4(a), 4(b) and 4(c) that the curves of volumetric strain rate changing with moisture content were similar when the samples only experienced dehydration shrinkage process. Specifically, the curves were straight down at the initial curing stage. At this stage, the capillary water inside the samples evaporated<sup>[21]</sup>, resulting in the shrinkage of pore volume that was the same as the volume of water loss. With the further decrease of moisture content, the air began to enter the pores of the sample<sup>[22]</sup>. As a result, the shrinkage of pore volume was smaller than the volume of water loss, and the shrinkage of pore volume gradually slowed down, and then the volumetric strain rate of the sample varied slowly with moisture content. With the continuous decrease of moisture content, the sample reached equilibrium in the curing humidity environment, and the sample volume no longer shrank. Under the curing humidity of 100%, as shown in Fig.4(d), samples W4 and W5 had water loss shrinkage. Samples W1–W3 with low water contents had moisture adsorption expansion, and the volume strain rate of samples increased linearly with moisture content, indicating that the volume expansion of samples was mainly controlled by moisture absorption.

Figure 5 shows the relationship between the final volume strain rate and the dry density of the sample and the curing humidity in the form of histogram. According to the data in Fig. 5 (a) and Table 4, for the samples W1–W3, when the initial moisture content  $w_0 < 17.22\%$  and the curing humidities were 33%,

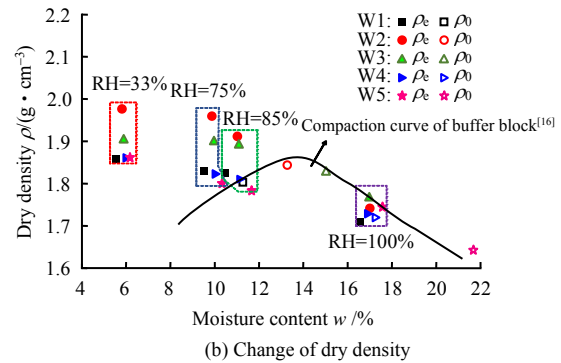


**Fig. 4** Variation of the volumetric strain rate of samples with moisture content

75% and 85%, the sample volume shrank and  $\beta = -4.13\% - -0.87\%$ ; in comparison, when the curing humidity was 100%, the sample volume expanded, and  $\beta = 3.50\% - 9.34\%$ . For the W4 and W5 samples, the initial moisture content  $w_0 \geq 17.22\%$ , and the volume shrinkage of the samples occurred to a certain extent at all curing humidity. The volume shrinkage decreased with the increase of curing humidity, and  $\beta = 0.31\% - 10.96\%$ . To sum up, it can be found that when the curing humidity was 100%, the sample (W4) with the initial moisture content of 17.22% had the minimum volume strain rate, which was 0.31%.



(a) Volumetric strain rate



(b) Change of dry density

**Fig. 5** Relationship between the changes of volumetric strain rate and dry density of samples and curing humidity

In Fig. 5(b), the solid points represent the dry density of the samples after curing equilibrium, and the hollow points represent the dry density of the newly pressed samples. These points correspond to the compaction curve of the hybrid buffer block, and the dotted box indicates the curing humidity. As can be seen from Fig. 5 (b), compared with the dry density of the newly pressed sample, when the curing humidities were 33%, 75% and 85%, the W1–W5 samples shrank due to water loss and the dry density increased. When the curing humidity was 100%, the W4 and W5 samples experienced dehydration shrinkage, and the dry density increased, while the W1–W3 samples experienced moisture adsorption expansion and the dry density decreased. The decrease of dry density would reduce the expansion and other properties of the sample [23], which was obviously detrimental to the engineering project.

In order to prevent the volume of bentonite–sand mixture samples from changing during buffer block curing, the most important point is to keep the moisture content in the sample constant. According to the above test results, when the curing humidity was 100%, the moisture content and volume of the sample with the initial moisture content of 17.22% changed the least. These two parameters can provide a reference for the selection of curing humidity and initial moisture content of the hybrid buffer block.

Figure 6 shows the surface images of the bentonite-sand mixture samples before and after curing. During curing, the reduction in moisture content would lead to the generation of suction and the shrinkage of soil samples. The proximity of soil particles to each other

would result in tensile stress inside the sample. When the tensile stress was greater than the tensile strength, cracks would occur<sup>[24]</sup>. As can be observed from Fig. 6, when the curing humidities were 33%, 75% and 85%, all the samples underwent the shrinkage process due to water loss, and the number of shrinkage cracks appearing on the sample surface was directly proportional to the initial moisture content of the sample, and inversely proportional to the curing humidity. When

the curing humidity was 100%, the monitoring data in Table 4 shows that the samples with low initial moisture content had moisture adsorption expansion, and the samples with high initial moisture content had water loss shrinkage. However, Fig. 6 shows that there was no obvious crack observed on the sample surface under this curing humidity, which proved that the high curing humidity was conducive to controlling the cracking and deformation of bentonite-sand mixture samples.


























Curing conditions	W1	W2	W3	W4	W5
Newly compacted samples	w=11.23% 	w=13.23% 	w=14.99% 	w=17.22% 	w=21.62% 
RH=33%	w=5.50% 	w=5.77% 	w=5.85% 	w=5.96% 	w=6.13% 
RH=75%	w=9.47% 	w=9.83% 	w=9.93% 	w=9.99% 	w=10.28% 
RH=85%	w=10.43% 	w=10.98% 	w=11.05% 	w=11.10% 	w=11.62% 
RH=100%	w=16.49% 	w=16.96% 	w=16.94% 	w=16.87% 	w=17.53% 

Fig. 6 Changes in the surface appearance of samples before and after curing (The moisture water content of newly compacted samples is initial moisture content, and the moisture water content of samples after curing is equilibrium moisture content)

### 3.3 Soil–water characteristic of samples

Soil moisture content is controlled by suction and environmental humidity, so the optimal curing humidity

can be predicted by the soil–water characteristic curve. In this work, the soil–water characteristic curve of bentonite-sand mixture with the dry density of 1.85 g/cm<sup>3</sup>



was measured by water vapour equilibrium method, as shown in Fig. 7. In order to obtain continuous soil–water characteristic curves, van Genuchten (vG) model<sup>[25]</sup> was used to fit the measured soil–water characteristic curves, as shown below:

$$w = \frac{w_r}{\left[1 + \left(\frac{\psi}{a}\right)^n\right]^{\frac{1}{n}}} \quad (3)$$

where  $w_r$  is the saturated water content;  $a$  and  $n$  are the fitting parameters; and  $\psi$  is the matrix suction.

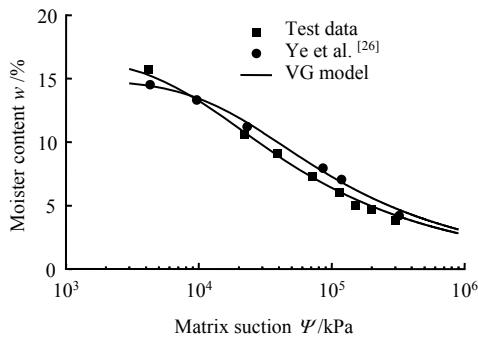


Fig. 7 Fitting of soil–water characteristic curves

The vG model parameters (see Table 5) used in this study refer to the test results presented by Ye et al.<sup>[26]</sup> with similar test conditions. The fitting correlation coefficient of the soil–water characteristic curve of bentonite–sand mixture was 0.994. Based on the fitting results of vG model, the optimal curing humidity of sample W1 was predicted to be 86.79%. This optimal curing humidity predicted by the soil–water characteristic curve was close to the optimal curing humidity measured by the test (i.e., 85%), which indicated that the optimal curing humidity predicted by the soil–water characteristic curve was consistent with the test results. Therefore, in the follow-up study on the optimal curing humidity of buffer blocks under different dry densities and moisture contents, the soil–water characteristic curve could be obtained by sampling from the block, and the optimal curing condition could be predicted according to the soil–water characteristic curve, and then the humidity range used in the test could be reduced. Meanwhile, the optimal initial moisture content of the block could be recommended according to the soil–water characteristic curve and relative humidity measured in the disposal repository.

Table 5 Model fitting parameters of soil–water retention curve

Data	Fitting parameters		Correlation coefficient $R^2$
	$a$ /kPa	$n$	
Present study	7 967.22	1.38	0.994
Ye et al. <sup>[26]</sup>	9 042.93	1.29	0.971

### 3.4 Change of thermal conductivity before and after curing

Crack development is one of the important indexes of block deterioration. But, as the width of the crack

generated during the drying and water loss of the block is usually less than 1 mm, the depth of cracks is hard to measure<sup>[3]</sup>, so it is difficult to evaluate the development of cracks inside the buffer block. Considering that the blocks are filled with air after cracks develop, there will be an air interface with heat resistance, thus reducing the thermal conductivity of the blocks. Therefore, in this paper, the thermal conductivity of bentonite-sand mixture samples before and after curing was measured, and the development of cracks in samples was quantitatively evaluated based on the empirical formula of heat conduction of bentonite-sand mixture.

As can be seen from Fig. 5, the water content and dry density of the samples changed after curing equilibrium, and some samples generated dry shrinkage cracks. According to the previous studies of Chen et al.<sup>[27]</sup> and Xu et al.<sup>[28]</sup>, the dry density and moisture content of samples had an impact on the thermal conductivity of samples. In order to further discuss the influence of cracks on thermal conductivity, this paper introduced the improved Johansen model<sup>[29]</sup> to predict the thermal conductivity of samples. It can be considered that this theoretical model was the relationship between dry density, moisture content, and thermal conductivity of samples without cracks.

Referring to the Johansen model<sup>[29]</sup> after the introduction of the Wiener parallel model by Zhang et al.<sup>[13]</sup>, the thermal conductivity of the sample can be calculated and the prediction equations are as follows:

$$\lambda_{m,p} = (\lambda_{sat} - \lambda_{dry}) K_e + \lambda_{dry} \quad (4)$$

$$\lambda_{sat} = \lambda_s^{(1-n')} \lambda_w^{n'} \quad (5)$$

$$\lambda_{dry} = \frac{0.135 \rho_d + 0.064}{\rho_s - 0.947 \rho_d} \quad (6)$$

$$K_e = 1.0 + \lg S_r \quad (7)$$

$$\lambda_s = \lambda_{ss} \phi_{ss} + \lambda_{sb} \phi_{sb} \quad (8)$$

where  $\lambda_{m,p}$  is the predicted value of thermal conductivity of the bentonite-sand mixture;  $\lambda_{sat}$  and  $\lambda_{dry}$  are the thermal conductivities when the saturation degree of the mixture is 100% and 0%, respectively;  $n'$  is the porosity of the mixture;  $K_e$  is the influence factor of saturation;  $\lambda_s$  is the thermal conductivity of the solid mixture;  $\lambda_w$ ,  $\lambda_{ss}$  and  $\lambda_{sb}$  are the thermal conductivities of water, quartz sand and bentonite, respectively, with values of 0.605 1, 7.700 0 and 2.000 0 W/(m · K);  $\phi_{ss}$  and  $\phi_{sb}$  are the volume fractions of quartz sand and bentonite in the mixture, respectively, and  $\phi_{ss} + \phi_{sb} = 1$ ;  $S_r$  is the saturation degree of the mixture; and  $\rho_d$  is the dry density of the mixture.

Figure 8 shows the comparison between predicted and measured values of the thermal conductivity of samples. In Fig. 8, the  $x$ -axis represents the measured average value of thermal conductivity, and the  $y$ -axis

represents the predicted value of thermal conductivity. "+10% line" and "-10% line" respectively indicate that the deviation between the predicted value of thermal conductivity and the measured average value is 10% (above the contour line is upward bias, and below the contour line is downward bias). As observed in Fig. 8(a), the predicted value of thermal conductivity of the newly pressed sample was close to the measured average value, and the deviation was less than 10%. Data points were randomly distributed on both sides of the isoline of predicted value and measured value, proving that the theoretical model could accurately predict the thermal conductivity of samples according to the moisture content and dry density of samples.

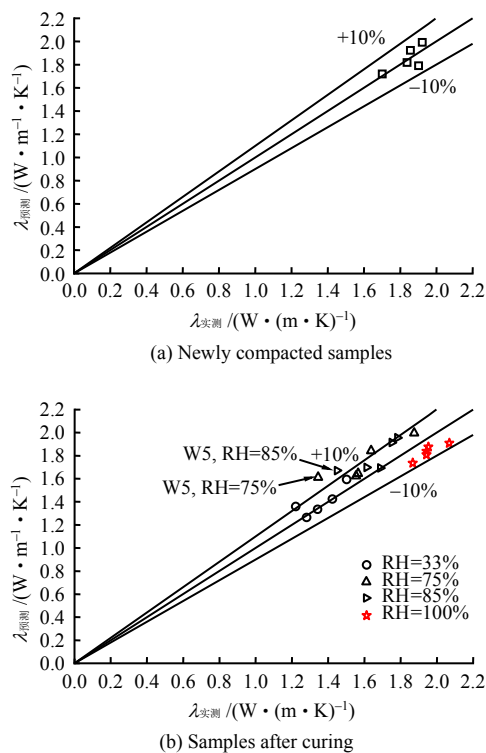


**Fig.8 Comparison between predicted and measured values of thermal conductivity of samples**

The difference between the measured and predicted values can be attributed to the cracks inside the sample. As can be seen from Fig. 8(b), when the curing humidities were 33%, 75% and 85%, the data points were mainly upward bias, that is, the predicted values of the thermal conductivity of the sample were all greater than the measured values. At this time, the sample lost water and shrank, and developed different dry cracks (see Fig. 6), indicating that the dry cracks would reduce the thermal conductivity of the sample. The cracks of the sample W5 were more evident when the curing humidities were 75% (thermal conductivity deviation was 22.36%) and 85% (thermal conductivity deviation was 13.38%), and the predicted value of thermal conductivity had a significant deviation from the measured value. Therefore, the deviation between the predicted value of thermal conductivity and the measured value could be used as an indicator to

evaluate the crack development of the sample. The larger deviation indicated that the samples had higher crack development. The samples (W5, 75%) with a deviation greater than 20% had a large number of cracks, and the width of the crack was large, where the crack was considered to be developed. In practical engineering, the heat conduction test can be used as a non-destructive testing method to evaluate the crack development of blocks, but the specific division of evaluation indexes needs further study in the future.

When the curing humidity was 100%, the data points were mainly downward bias, that is, the predicted values of the thermal conductivity of the samples were all smaller than the measured values, as a result of that the samples became more uniform due to the adjustment of moisture inside the sample during the curing process. The above results showed that the thermal conductivity of the sample was reduced by dry cracks. The more the cracks developed, the more significant the decrease degree was. At the same time, the thermal conductivity of the sample could be improved by high humidity curing (RH = 100%).

## 4 Conclusions

(1) When the curing humidities were 33%, 75% and 85%, all the samples showed drying loss of water and volume shrinkage, and dry shrinkage cracks occurred on the surface of the samples. When the curing humidity was 100%, the moisture adsorption expansion occurred in the sample with the low initial moisture content (11.23%–14.99%), and the water loss shrinkage occurred in the sample with the high initial moisture content (17.22%–21.63%). In this case, when the curing humidity was 100%, the moisture content and volume change of the sample with the initial water content of 17.22% were the minimum (0.35% and 0.31%, respectively), which was considered as the potential optimal curing condition for blocks.

(2) The moisture evolution of the bentonite-sand mixture compacted sample during curing was controlled by suction. The optimal curing humidity could be predicted by the soil–water characteristic curve of the sample. And the initial moisture content suitable for blocks could be predicted by environmental humidity and soil–water characteristic curve.

(3) The crack development of the mixture samples could be quantitatively evaluated by comparing the measured thermal conductivity results with those determined by the empirical formula. Drying cracks would reduce the thermal conductivity of the sample. The larger the deviation between the measured value and the predicted value of the thermal conductivity, the higher the crack development of the sample. When the deviation was greater than 20%, the crack was considered to be developed.

## References

- [1] Svensk Kärnbränslehantering A B. Programme for research, development and demonstration of methods for the management and disposal of nuclear waste[R]. [S. l.]:

- Svensk Kärnbränslehantering AB, 2001.
- [2] YAN Ming, WANG Xue-wen, ZHANG Hu-yuan. Current status of preparing buffer/backfill block in HLW disposal abroad[J]. *World Nuclear Geoscience*, 2014, 31(Suppl. 1): 327–330.
- [3] TAN Y, ZHANG H Y, HE D J, et al. Deterioration of exposed buffer block: desiccation shrinkage and cracking[J]. *Bulletin of Engineering Geology and the Environment*, 2019, 78(7): 5431–5444.
- [4] TORBJÖRN S. Investigation of backfill candidate materials[R]. [S. l.]: Svensk Kärnbränslehantering AB, 2014.
- [5] TORBJÖRN S, BÖRGESSON L, DUECK A. KBS-3H description of buffer tests in 2005–2007[R]. [S. l.]: Svensk Kärnbränslehantering AB, 2008.
- [6] PETER E. Investigation of alternatives to the buffer protection[R]. [S. l.]: Svensk Kärnbränslehantering AB, 2018.
- [7] WANG J, CHEN L, SU R, et al. The Beishan underground research laboratory for geological disposal of high-level radioactive waste in China: planning, site selection, site characterization and in situ tests[J]. *Journal of Rock Mechanics and Geotechnical Engineering*, 2018, 10(3): 411–435.
- [8] XIA Zi-tong, WU Shao-xu, ZHANG Bao-zeng, et al. Environmental impact report of China Beishan underground laboratory construction project[R]. Beijing: Beijing Research Institute of Uranium Geology, 2020.
- [9] LARS-ERIK J. Characterization of backfill candidate material, IBECO-RWC-BF Baclø Project–Phase3[R]. [S. l.]: Svensk Kärnbränslehantering AB, 2010.
- [10] BENOIT G, HEREIG R M, HANSPETER W. FE/LUCOEX: Design criteria for bentonite block manufacturing and emplacement in an underground facility[C]/LUCOEX Conference and Workshop: Full-scale Demonstration Tests in Technology Development of Repositories for Disposal of Radioactive Waste. [S. l.]: [s. n.], 2015.
- [11] JUVANKOSKI M. Buffer design 2012[R]. [S. l.]: Posiva Oy, 2013.
- [12] ZHANG Hu-yuan, ZHANG Guo-chao, YU Rong-guang, et al. Spatial distribution and anisotropy in swell of compacted bentonite-sand block for HLW buffer barrier[J]. *Chinese Journal of Rock Mechanics and Engineering*, 2019, 38(Suppl.2): 3469–3480.
- [13] ZHANG Hu-yuan, ZHAO Bing-zheng, TONG Yan-mei. Thermal conductivity and uniformity of hybrid buffer blocks[J]. *Rock and Soil Mechanics*, 2020, 41(Suppl.1): 1–9, 18.
- [14] TAN Y, ZHANG H Y, ZHANG T W, et al. Anisotropic hydro-mechanical behavior of full-scale compacted bentonite-sand blocks[J]. *Engineering Geology*, 2021, 287: 106093.
- [15] ZHU Li-ping, ZHANG Hu-yuan, TAN Yu, et al. The determination of the optimal bentonite-sand ration based on fuzzy integrated evaluation[J]. *Journal of Lanzhou University (Natural Sciences)*, 2018, 54(3): 310–316.
- [16] WANG Xue-wen. Research on compacting properties of buffer block for HLW disposal[D]. Lanzhou: Lanzhou University, 2017.
- [17] ZENG Hao, TANG Chao-sheng, LIN Chang-li, et al. Interfacial friction dependence of propagation direction and evolution characteristics of soil desiccation cracks[J]. *Chinese Journal of Geotechnical Engineering*, 2019, 41(6): 1172–1180.
- [18] YOUNG J F. Humidity control in the laboratory using salt solutions—a review[J]. *Journal of Applied Chemistry*, 1967, 17(9): 241–245.
- [19] China Building Materials Academy. GB/T35166—2017 Hygrothermal performance of building materials and products—determination of moisture adsorption/desorption properties in response to humidity variation[S]. Beijing: Standards Press of China, 2017.
- [20] DAO Minh-huan, LIU Qing-bing, HUANG Wei, et al. Study on desiccation–shrinkage characteristic and shrinkage cracking mechanism of bentonite and sand mixtures[J]. *Rock and Soil Mechanics*, 2020, 41(3): 789–798.
- [21] CHEN P, LU N. Generalized equation for soil shrinkage curve[J]. *Journal of Geotechnical and Geoenvironmental Engineering*, 2018, 144(8):04018046.1–04018046.10.
- [22] CHEN Pan, XIANG Rui, WEI Xiao-qi, et al. Equation for soil shrinkage curve of clay considering soil-water adsorption effect[J]. *Journal of Shanghai University*, 2020, 54(8): 866–872.
- [23] ZHANG Hu-yuan, CUI Su-li, LIU Ji-sheng, et al. Experimental study of swelling pressure of compacted bentonite-sand mixture[J]. *Rock and Soil Mechanics*, 2010, 31(10): 3087–3095.
- [24] NAHLAWI H, KODIKARA J K. Laboratory experiments on desiccation cracking of thin soil layers[J]. *Geotechnical & Geological Engineering*, 2006, 24(6): 1641–1664.
- [25] VAN GENUCHTEN M TH. A closed-form equation for predicting the hydraulic conductivity of unsaturated soils[J]. *Soil Science Society of America Journal*, 1980, 44(5): 892–898.
- [26] YE Wei-min, SHEN Miao, CHEN Bao, et al. Water retention characteristics of highly compacted sand-GMZ01 bentonite mixtures at fixed temperatures[J]. *Journal of Engineering Geology*, 2013, 21(3): 385–390.
- [27] CHEN Hang, ZHANG Hu-yuan, GUO Yong-qiang, et al. Measurement and prediction of thermal properties of bentonite-sand mixtures as buffer backfilling materials for high level radioactive waste[J]. *Chinese Journal of Rock Mechanics and Engineering*, 2014, 33(Suppl.2): 4312–4320.
- [28] XU Yun-shan, SUN De-an, ZENG Zhao-tian, et al. Experimental study on aging effect on bentonite thermal conductivity[J]. *Rock and Soil Mechanics*, 2019, 40(11): 4324–4330.
- [29] JNHANSEN O. Thermal conductivity of soils[D]. Trondheim: [s. n.], 1977.